Hybrid speed bump-PV-battery-grid power generation in a smart grid environment

Oluwafemi Oni, *Robert Thokozani* Skhosanaa, and *Omowunmi Mary* Longe*

Department of Electrical & Electronic Engineering Science, University of Johannesburg. Johannesburg, South Africa

Abstract. To meet the growing demand for clean energy and improved energy availability factor in South Africa, various solutions are being proposed from academia and industry. Therefore, in this study, a non-conventional method of generating clean energy was designed and constructed. The proposed system harnesses the kinetic energy of vehicles driving over speed bumps and converts it to electrical energy using a generator. This energy is supplemented with the energy generated from solar PV panels to provide a sustainable power supply for traffic and streetlights. The system is further designed to operate with a grid connection as a backup. An interface was further created to give real-time monitoring of electric power generation and consumption. The setup is also suitable for areas with limited/no access to electricity, and in the case of loadshedding. The results obtained during the testing of this prototype demonstrate the effectiveness of the system to provide a reliable source of electricity for street and traffic lights to ensure safety on the roads and avoidance of traffic congestion during loadshedding. The prototype is scalable to meet future power demands and feed into the grid in a smart grid environment.

1 Introduction

Energy crisis is becoming a serious problem in South Africa as a result of a shortage in the generating capacity and 58% energy availability factor (EAF) from the utility provider [1]. Besides, energy consumption has grown considerably due to the increasing population and additional loads [2]. The country's energy consumption is largely dependent on non-renewable sources such as natural gas, coal, and oil [3], which have caused significant atmospheric and environmental pollution, resulting in phenomena such as climate change, and other greenhouse gas effects. Given the current global economic uncertainty and the fluctuation of energy costs as a result of limited resources, it is critical to prioritize the usage of renewable energy sources for highly important tasks in our day-to-day living.

Emerging solution focuses on decentralized renewable energy (DRE) power production systems [4]. This can play an essential role in combating the low EAF in South Africa's urban and rural areas. Main reason because the decentralized solutions can be more cost-

* Corresponding author: omowunmil@uj.ac.za

effective, and highly reliable than the central grid for delivering power to remote, low-density or urban areas. Battery storage with a renewable energy source can further be incorporated to build a hybrid DRE power supply system. In comparison to the utility grid or single sourced energy systems, hybrid DRE systems have numerous advantages, including increased power supply reliability, environmental damage mitigation, smaller component sizes, and possibly lower unit energy costs. Solar-photovoltaic-based hybrid systems are a viable option in many South African cities since solar radiation is abundant in most of the provinces.

With the fast urbanization and increase in the number of internal combustion engine cars, urban transportation is a major contributor to increase in energy consumption, triggering a series of problems such as unclean energy consumption, high CO_2 emissions and air pollution [5]. Other facilities needed for a well mapped out urban centre are a well-lit streetlight, and a functional traffic controlling lights. However, a non-functioning streetlights and traffic lights in various regions have been cumulated to a rise in crime rates and accidents, particularly affecting pedestrians, including workers and students. Streetlights and traffic lights serve to enhance road safety by illuminating the streets and providing a right of pass, thereby rendering individuals more conscious of their environment. Statistics reveal that absence of adequate street and traffic lighting elevates the likelihood of robbery and vehicular accidents [6]. The use of renewable energy technology has shown to be a long-term answer to these transportation industry's problems.

Traffic is one of the most energy-intensive parts of human activities in the urban environment, and it is also one of the most wasteful. It was noted that just 30 percent of the fuel capacity is used to transfer kinetic energy to the vehicle during traffic, and most of this energy is lost in decelerating stages by braking. With over 30% of the population utilizing automobiles for daily activities, one possible avenue for alternate energy generation is the conversion of road friction generated by traffic calming devices such as speed breakers, speed humps, cushions, and speed charts. These vertical deflection devices are commonly used to reduce the amount of motor vehicle traffic and improve safety conditions by imposing a low-speed restriction of less than 40 km/h. These devices are needed mostly at decelerating locations, for example, urban road and pedestrian crossings, and important road exits because it enables the best possible mix of increased road safety and compensation of carbon emissions.

Recent research studies have attempted to identify new environmentally friendly energy sources that are both profitable and efficient. Roadway speed bumps are promising candidates and have been researched upon because of their constant exposure to diverse energy sources for energy gathering resources [7-10]. As a result, there is a growing interest in energy harvesting by collecting squandered unconventional sources and transforming them to a usable energy form. PV solar radiation wind hybrid power generation was used in [11] for street lighting, and heat energy harvesting from pavements was proposed in [12]. The aforementioned sources of energy are dissipated into the pavement as strain and thermal energy. These technologies were proposed for the roadside infrastructure network and to feed smart transportation systems that control traffic and health monitoring systems, electrical signs and lighting, etc. The decrease in different electronics circuitry size and power consumption due to recent advances in complementary metal-oxide semiconductors has further motivated researchers to develop new energy harvesting devices, such as electrohydrodynamic (EHD) devices that can be used to generate power from a variety of sources, including vibrations, air flow, and even human motion.

Therefore, in this paper, an embedded design of a speed bump and PV system were proposed for power generation for streetlights and traffic lights. The study also included a battery backup with availability for grid input. The result from the experimental testing of the design were recorded. The main contribution comes in the design of the hybrid DRE

and implementation of internet of things (IoT) database using ThingSpeak for online monitoring of the design. The final design prototype was built to generate a minimal amount of power of up to 10 watts. This power could be used to power traffic lights, streetlights, or even small electronic devices. And thus demonstrate the feasibility of harnessing energy from road speed breakers and incorporating it into daily usage for traffic lighting and streetlight.

2 The photovoltaic solar cell current-voltage characteristic curve

The current-voltage (I-V) characteristic curves of a solar cell demonstrate the current and voltage properties of a given PV cell, module, or array, by providing its electrical features. This data gives a thorough examination of the cell's efficiency and capacity to convert solar energy. Understanding the I-V properties of a solar panel or cell, particularly P_{max}, is critical for determining its performance and solar efficiency. The PV solar cells convert the sun's radiant radiation directly into electrical energy. Solar energy conversion has become an increasingly essential element of the mix of renewable energy sources because of the growing need for clean energy and the sun's capability as a renewable energy source. As a result, consumer interest in efficient solar cells that convert sunlight directly into power is increasing more rapidly than ever. Because solar cells generate direct current (DC) electricity, we can create I-V curves for solar cells that represent the current versus voltage for a photovoltaic device [13]. The current-voltage (I-V) properties of a typical silicon PV cell is shown in Figure 1 during normal operating conditions [14]. To calculate the power output of a solar panel or cell, one needs to multiply its output current and voltage (IV). By performing this multiplication for each voltage point between short-circuit and open-circuit conditions, a power curve can be obtained for a specific radiation level [15].

A PV cell's I-V curve is the superposition of the dark I-V curve of the solar cell diode and the light-generated current. The light causes the I-V curve to drop down towards the fourth quadrant, where power may be recovered from the diode. Illuminating a cell increases the typical dark currents in the diode, causing the diode law to become Equation 1, which when rearrange will give the voltage relationship shown in Equation 2.

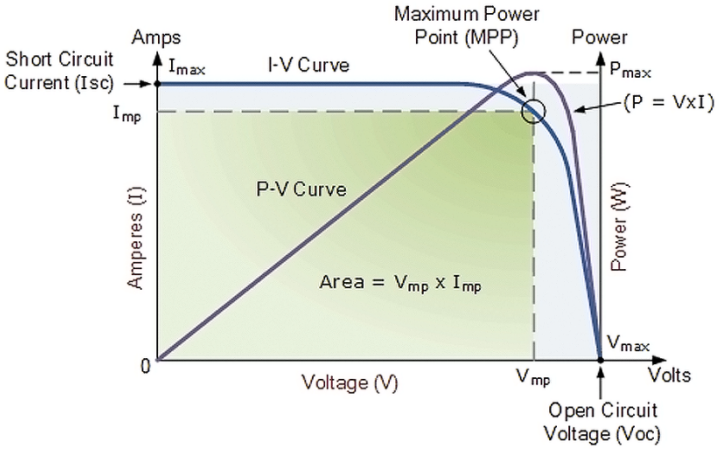

Fig. 1. A solar cell I-V characteristics curve [15].

$$I = I_0[\exp\left(\frac{qV}{nkT}\right) - 1] - I_L; \quad (1)$$

$$V = \frac{nkT}{q} ln(\frac{I_L - I}{I_0}). \quad (2)$$

where I_L = light generated current.

The relationship between the output current and voltage of a photovoltaic array summarizes its electrical properties. The quantity and strength of solar insolation, also known as solar irradiance, determines the level of output current (I), while the operational temperature of the solar cells impacts the output voltage (V) of the cell array.

3 Roller design model

This study proposed a methodology for generating electricity by utilizing a roller as shown in Figure 2 [7] placed between a speed bump and a specialized grip on the speed breaker. When a vehicle drives over the speed breaker, the roller is rotated, thereby turning the shaft of a generator to produce electrical energy. Mathematical formulas were employed in this study to determine the amount of electricity generated. Firstly, the simple circuits of the generator with the internal resistance and inductance (R_i and L_i) are respective shown in Figure 3. The load resistor, which is the point of harvesting the generated power is also shown and denoted as R_L. This diagram denotes an ideal generator, i.e., with a negligible value of L_i. According to the electromagnetic model of the generator in Figure 3, the electromotive voltage and electromagnetic torque is shown in Equations 3 and 4 respectively. Other parameters are the induced electromotive voltage V_{gen}, back electromotive voltage constant K_{gen}, rotational speed of the generator ω_{gen}, torque constant K_T, and external current i_{gen}. At low frequency of f, the internal inductance L of the geneator is usually small, that is, $FL < (R_i + R_L)/2\pi$. Therefore, the internal inductance L can be negligible. The final torque of the generator is given in equation 5 [16].

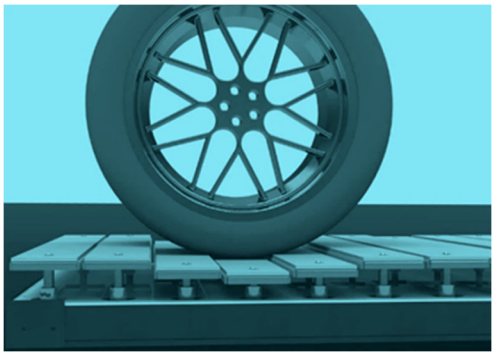

Fig. 2. Prototype of a speed bump design for energy recovery [7].

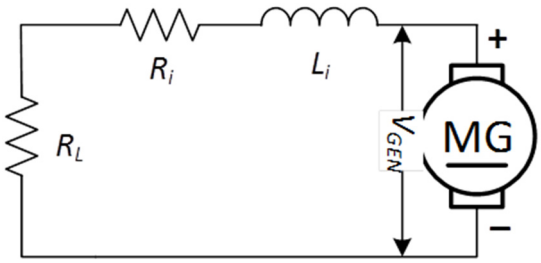

Fig. 3. Simplified model of a dc generator for the speed bump converter.

$$V_{gen} = K_{gen}\omega_{gen}; \quad (3)$$

$$T_{gen} = K_T i_{gen}; \tag{4}$$

$$T_{gen} = K_T \frac{V_{gen}}{R_i + R_L} = \frac{K_T K_{gen} \omega_{gen}}{R_i + R_L}. \tag{5}$$

This study offered a method in which a roller is placed between a speed bump and a grip is provided on the speed breaker such that when a vehicle drives over the speed breaker, the roller is turned. The generator produces electricity when the generator's shaft spins. The torque power relationship is given in equation 6. The angular speed of the generator equation is given in equation 7 while equation 8 gives the power equation.

$$\tau = P\omega; \tag{6}$$

$$\omega = \frac{2\pi N}{60}; \tag{7}$$

$$P = VI \quad , \tag{8}$$

where: P is the power generated (output power), ω is the angular speed of the motors, τ is the torque of the motors. N is the rotational speed of the motors, V is voltage produced by the motors, and I is the current computed from each subsystem.

4 Design prototype

The diagram in Figure 4 shows how each subsystem was integrated with the system. It consists of the speed bump arrangements, different relays, solar PV, grid electricity and different peripherals working concurrently to provide an efficient system.

The speed breaker is a spring that is supported at both ends, which can create linear motion. Pistons are placed beneath the speed breaker, and when a vehicle drives over it, the pistons are pushed down. This movement allows the piston to compress the oil beneath it, which is then transported to an accumulator. The accumulator is connected to a motor that generates torque from the compressed oil. As the roller turns the shaft of the DC motor, the torque is converted into electrical energy. Therefore, the kinetic energy produced by the motor's spinning is transformed into electrical energy, which is then stored in a battery.

LDR (light dependent resistor) was used to make sure that lights go on at a certain time. A timer switch is required to achieve this through the use of a timer switch.

The system is designed to made used of three sources of power namely, roller speed bump power generated via kinetic energy harvesting, solar PV, and the grid. The system is also equipped with battery bank. The Arduino used has been programmed with order of preference in selecting the sources. The relays help in the switching between these sources. Power generated via speed bump and the Solar PV are the main source of power for this system. They directly charge the battery, and thus further supply the street and traffic lights. The grid serves as a backup in a rare case of when there is no supply of power through either of the primary sources.

According to technical sources, it has been reported that the ESP8266 module has the capability to act as a host for an application or alternatively, it can offload all Wi-Fi IEEE 802.11 standard networking functions from another application processor. It has been noted that every ESP8266 module is pre-programmed with an AT command set firmware, which implies that when connected to an Arduino board, it offers similar Wi-Fi capabilities as a Wi-Fi Shield. Furthermore, the ESP8266 module is recognized as a highly cost-effective board and has a large and continuously expanding community of users.

The most important component is the Arduino MEGA because it is the one that controls every subsystem. Arduino mega 2560 serial monitor results from the grid, solar, battery, and roller. Results generated through this monitoring are shown in Figure 5. Each subsystem is represented by its voltage, current and power. This Serial Monitor results show the real-time current, voltage, and power of the different subsystems. The first value is current, the middle value is voltage, and the final value is power. The battery stays the same for most part of the testing because the roller and solar take time to charge the battery. The values that change a lot throughout the experiment are for the roller because cars pass over the roller at different times, with different speeds and weights. The polycrystalline solar panels used are two 1.5 V 0.25 W with 14%-16% efficiency placed on top of the streetlights.

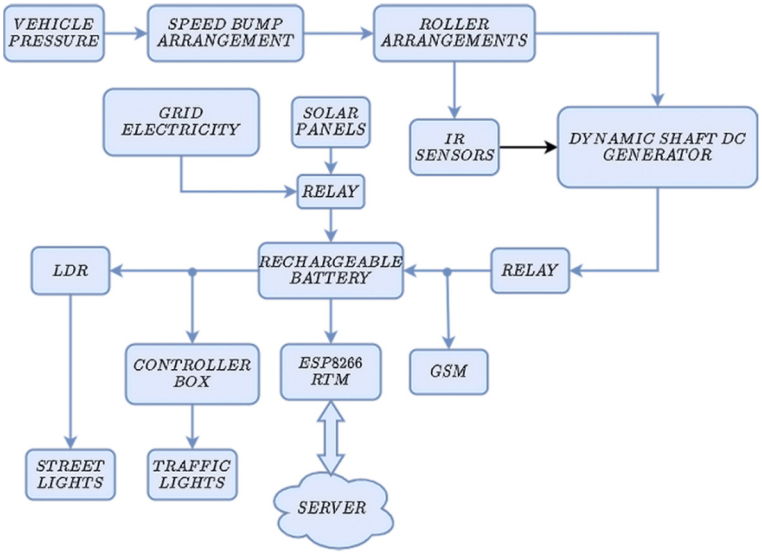

Fig. 4. Design of database table.

Roller,0.21,1.69,0.36	Roller,0.24,1.69,0.40
Solar,0.29,0.44,0.13	Solar,0.24,0.44,0.10
Grid,0.29,0.47,0.14	Grid,0.32,0.47,0.15
Battery,0.26,12.39,3.27	Battery,0.32,12.39,3.92
Roller,0.24,1.69,0.40	Roller,0.21,1.69,0.36
Solar,0.26,0.44,0.12	Solar,0.32,0.44,0.14
Grid,0.32,0.47,0.15	Grid,0.29,0.47,0.14
Battery,0.29,12.39,3.60	Battery,0.32,12.39,3.92
Roller,0.21,1.69,0.36	Roller,0.21,1.69,0.36
Solar,0.26,0.44,0.12	Solar,0.29,0.44,0.13
Grid,0.26,0.47,0.12	Grid,0.34,0.48,0.16
Battery,0.32,12.39,3.92	Battery,0.34,12.39,4.25
Roller,0.26,1.69,0.45	Roller,0.18,1.69,0.31
Solar,0.29,0.44,0.13	Solar,0.29,0.44,0.13
Grid,0.32,0.47,0.15	Grid,0.34,0.47,0.16
Battery,0.29,12.39,3.60	Battery,0.32,12.39,3.93
Roller,0.21,1.69,0.36	Roller,0.18,1.69,0.31
Solar,0.26,0.44,0.12	Solar,0.32,0.44,0.14
Grid,0.29,0.47,0.14	Grid,0.34,0.47,0.16
Battery,0.32,12.39,3.92	Battery,0.32,12.39,3.92

Fig. 5. Serial monitor results.

5 Testing and results

Figure 6 shows the results for the roller Speed Bump Roller mechanism from the serial monitor. A minimum of four results were selected. Each time a car passes over the ramp, the current and voltage are recorded and then the power is computed from the product of the two values.

The IoTs aspect of this research involves the use of web-based tools to monitor the data generated from the implementation of this design. The website displays the different results of the subsystems. On the left tab of the website, all the components displayed are from the roller, solar and Grid, the battery Bank, notifications, and cost. Clicking on one of the tabs will display the required results of that specific system. For the solar, the amount of power generated from the sun is going to be shown and when the grid electricity is on, the results related to the grid will be shown. Notifications happen when there is a fault in the system and display a notification when the energy in the battery is depleted. This part of the experiment uses the GSM SIM 800L to send notifications to the user when there is a fault in the system as shown in Appendix B and C. The user needs to be notified through a fast-messaging system and the GSM 800C was used to send messages to the user when there is a fault in the system e.g., when there is no current flowing in the circuit a message will be sent, which as well signifies a fault in the system.

The following results were taken using ThingSpeak during the testing of all the different subsystems. The first results, shown in Figures 7a and 7b, is for the roller speed bump. The data were taken in July and the second results were taken in October, the straight line in between these dates does not display a trend, it is a space in time where no results were taken. The results displayed are only for one reading, although multiple readings were taken which increases the reliability of the data taken from experiments.

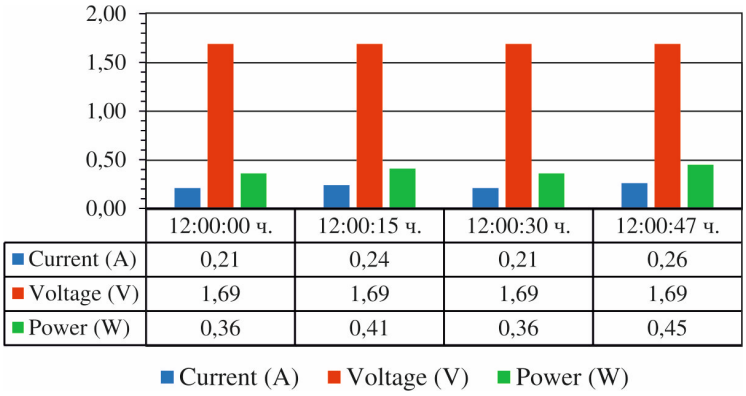

	12:00:00 ч.	12:00:15 ч.	12:00:30 ч.	12:00:47 ч.
Current (A)	0,21	0,24	0,21	0,26
Voltage (V)	1,69	1,69	1,69	1,69
Power (W)	0,36	0,41	0,36	0,45

Fig. 6. Roller Mechanism result showing the results (V-I-P vs Time) results from serial monitor.

(a) (b)

Fig. 7. Roller speed bump ThingSpeak showing (a) voltage and (b) current results.

During the usage of Solar PV, data were taken based on the reading on the system display for voltage and current at different time interval as shown in Figure 8 from experiments. The value taken was low because of the size of the polycrystalline Solar panel that was used. As this project is scalable, increasing the power output is possible with the increase in the sizing of the solar panel. Further results were taken using ThingSpeak during the testing of all the different subsystems when Solar PV system was connected. The data were taken in October at different time interval as shown in Figures 9a and 9b. The line in between also signifies dates and time where no results were taken. The results displayed are only for one reading, although multiple readings were taken which increases the reliability of the data taken from experiments.

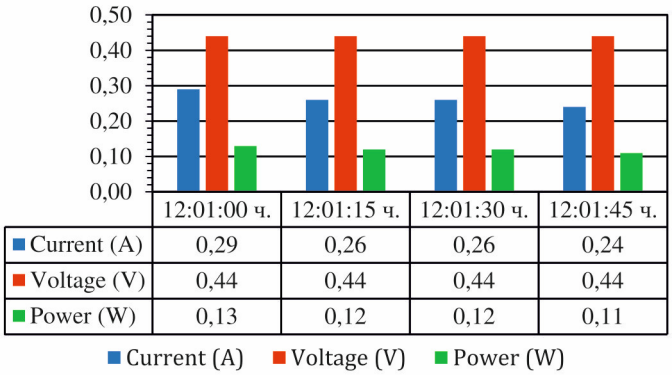

	12:01:00 ч.	12:01:15 ч.	12:01:30 ч.	12:01:45 ч.
Current (A)	0,29	0,26	0,26	0,24
Voltage (V)	0,44	0,44	0,44	0,44
Power (W)	0,13	0,12	0,12	0,11

Fig. 8. Solar PV results from serial monitor (V-I-P vs Time).

Figure 10 shows the results for the grid electricity from the serial monitor. A minimum of four results were selected. The current and voltage are recorded and then the power is computed from the product of the two values.

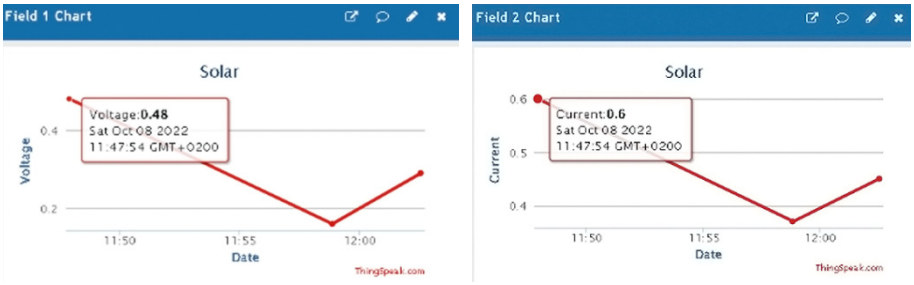

(a) (b)

Fig. 9. Solar PV (a) voltage and (b) current vs time results.

Figure 11 shows the results for the battery bank from the serial monitor. The current and voltage are recorded and then the power is computed from the product of the two values. A minimum of four results were selected and the results show that the battery was being used since the power values increased after it was charged by the roller and solar energy. The exterior and interior of the prototype hybrid power generator are presented in Figures 12a and 12b. The figure includes components used in this prototype are: Rechargeable Battery, Arduino MEGA 2560, Polycrystalline Solar Panel, LED Lights, IR Sensors, GSM 800L, Current Sensors, Relays and boost converters, Breadboard, and connecting cables.

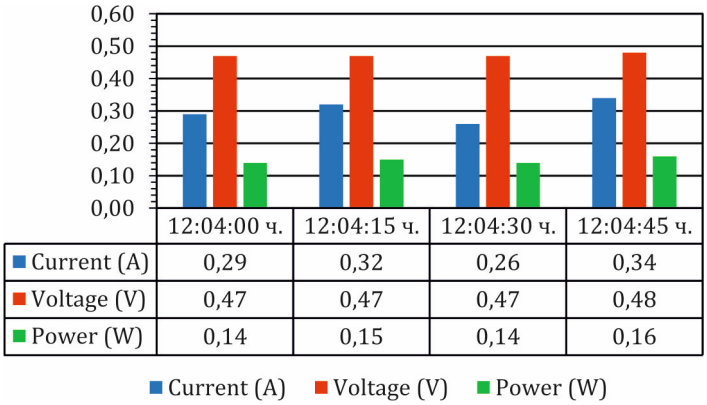

	12:04:00 ч.	12:04:15 ч.	12:04:30 ч.	12:04:45 ч.
Current (A)	0,29	0,32	0,26	0,34
Voltage (V)	0,47	0,47	0,47	0,48
Power (W)	0,14	0,15	0,14	0,16

Fig. 10. Graph showing results for grid electricity (V-I-P vs Time).

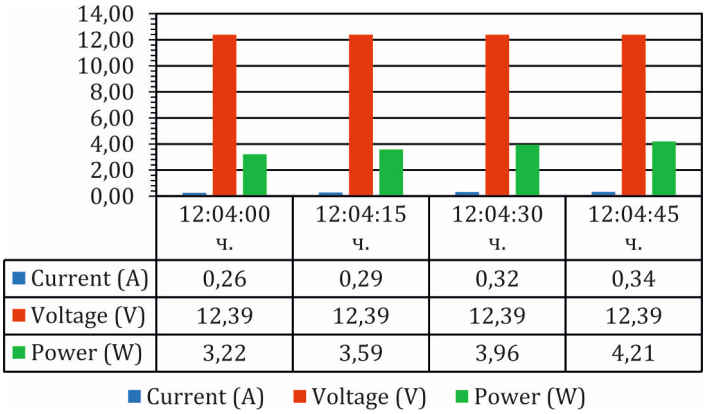

	12:04:00 ч.	12:04:15 ч.	12:04:30 ч.	12:04:45 ч.
Current (A)	0,26	0,29	0,32	0,34
Voltage (V)	12,39	12,39	12,39	12,39
Power (W)	3,22	3,59	3,96	4,21

Fig. 11. Graph showing results for the battery bank (V-I-P vs Time).

The testing of the prototype using a toy car is shown on Figure 13. As soon as the truck passes the 1st IR Sensor, it will detect the truck and cause the roller to move, and it stops when the car has passed over the 2nd IR sensor. The speed at which the car passes the roller speed bump determines the amount of power generated at the outside end of the generator. The output, being a small prototype, is made to be in dc since all the needed loads are in dc. This way, losses are minimized because if converted to AC, the losses due to the IGBTS or diode switches will lead to a reduction in the output power for the streetlight and traffic light load. The results presented in this work contribute to the fact that hybrid energy generation would play a big role in the energy generation for the future smart grid both in rural and urban areas as earlier asserted by [7, 8, 11, 12, 17, 18]. This work on a large scale can feed into the grid to increase grid reliability and contribute to improved EAF in the country and reduce hours of loadshedding in the areas where hybrid speed bump-PV-Battery-Grid systems are in the country. The deployment of this solution could contribute to the Minister of Electricity's goal of achieving 75% EAF [19].

The results generated during the IoTs testing of this prototype are shown in the Appendix section. The ThingSpeak website used is shown in Appendix A. This diagram shows different subsystem as combined. And being equipped with fault tracking and report capabilities, the diagram in Appendix B shows the notification which is directly sent to the user via SMS. The diagram in Appendix C shows the exact location of faults or report on the usage of the battery.

a)

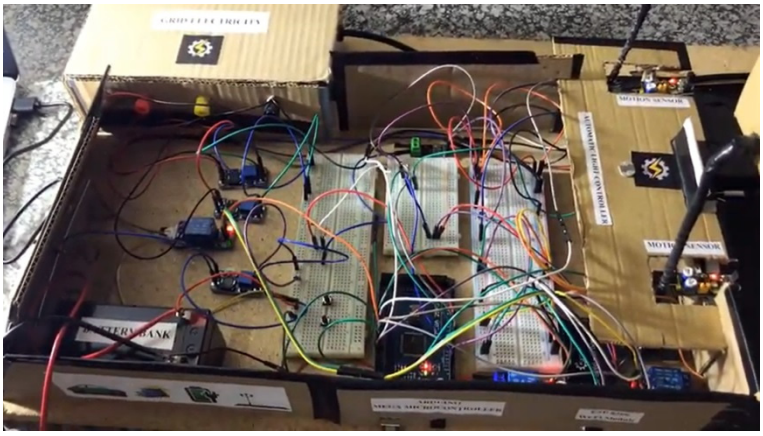

b)

Fig 12 Exterior (a) and interior (b) of the designed solar PV-speed bump hybrid power generator prototype.

Fig. 13. A toy car going over the speed bump.

The prototype costed about R2400 (approximate $125) as at the time of writing this paper. Large scale production of the device would reduce the per unit cost of the system with good return-on-investment for the company that would manufacture them.

6 CONCLUSION

In this paper, an embedded design of a speed bump-PV-Battery-Grid clean power generation were proposed for streetlights and traffic lights. This system is designed to recover energy from traffic on speed bumps. The usefulness of this design is to help alleviate over-reliance on the grid, increase security at night on the roads and improve grid EAF from its present state of 58%. The performance of the designed prototype has been analyzed by carrying out a serial monitoring of the device using ThingSpeak. ThingSpeak is a web base tool link with the design to give a real time data capturing of the device to mimic a smart grid environment. The test carried out confirmed that the prototype, which was built to supply power for street and traffic lights, can also be applied for monitoring traffic or highway indication systems, and for infrastructure utilities such as electrical signage, lighting etc. The practical implementation of this design on South African roads will come in handy in reducing the traffic congestion during loadshedding and save time taken by commuters to get to their destinations during loadshedding. It will also play a crucial role in augmenting security at night in our communities and improving the quality of life by artificially prolonging the duration of daylight hours, thereby facilitating extended hours for commercial activities and improved economy.

Some of the limitations of the study that can be mitigated in future designs include use of monocrystalline solar panels instead of polycrystalline solar panels, and use of at least a raspberry-pi instead of an Arduino Uno microcontroller. Also, more budget should be given to practically deploy the proposed solution on our roads.

References

1. O. Analytica, "Eskom bailout will not solve South Africa power crisis," Emerald Expert Briefings, no. oxan-db, (2023).
2. M. C. Udeagha, N. Ngepah, Econ. Change and R., **55**, 3, pp. 1767-1814, (2022).
3. B. Büscher, S. Koot, L. Thakholi, Envrnmt and Planning E: Nat. and Space, p. 25, (2022).
4. V. Harish, N. Anwer, and A. Kumar, Sust. Energy Tech and Assmnts, **52**, p. 102032, (2022).
5. K. A. Collett, S. A. Hirmer, H. Dalkmann, C. Crozier, Y. Mulugetta, M. D. McCulloch, Energy Strat. Reviews, **38**, p. 100722, (2021).
6. V. N. Sumantri, A. I. Rifai, F. Ferial, Citizen: Jurnal Ilmiah Multidis. Indnsia, **2**, no. 5, pp. 703-711, (2022).
7. A. Pirisi, M. Mussetta, F. Grimaccia, R. E. Zich, IEEE Trans. on Int. Trans. Sys., **14**, no. 4, pp. 1983-1991, 2013.
8. I. R. R. KranthiMadala, M. F. Shaik, Recnt Dev in Electr and Coms Sys, **32**, pp. 475-483, (2023).
9. M. Gholikhani, R. Nasouri, S. A. Tahami, S. Legette, S. Dessouky, A. Montoya, Applied Energy, **250**, pp. 503-511, (2019).
10. M. Sun, W. Wang, P. Zheng, D. Luo, Z. Zhang, Sensors and Actuators A: Phy, **323**, p. 112648, (2021).

11. W. R. Nyemba, S. Chinguwa, I. Mushanguri, and C. Mbohwa, Procedia Manufac. **35**, pp. 285-290, (2019).
12. A. Dawson, R. Mallick, A. G. Hernandez, P. K. Dehdezi, Climate Change, Energy, Sust. and Pavements, pp. 481-517, (2014).
13. A. Orioli, Renewable Energy, **145**, pp. 725-743, (2020).
14. J. M. Greulich et al., Solar Energy Mat. and Solar Cells, vol. 248, p. 111931, (2022).
15. S. A. Afghan, H. Almusawi, and H. Geza, "Simulating the electrical characteristics of a photovoltaic cell based on a single-diode equivalent circuit model," in MATEC Web of Conferences, 2017, **126**: EDP Sciences, p. 03002. (2017)
16. L. Wang, P. Todaria, A. Pandey, J. O'Connor, B. Chernow, L. Zuo, "An electromagnetic speed bump energy harvester and its interactions with vehicles," IEEE/ASME Trans. on Mech., **21**, no. 4, pp. 1985-1994, (2016).
17. L. Olatomiwa, A. A. Sadiq, O. M. Longe, J. G. Ambafi, K. E. Jack, T. A. Abd'azeez, S. Adeniyi, Energies, vol. 15, no. 9554, (2022).
18. R. Gilbert, O. M. Longe, “A Feasibility Study on Optimal RES Microgrid Design for Rand West Municipality,” in IEEE Power Africa Conference (PAC), Nairobi, Kenya, 2020, pp. 1-5. (2020)

    C. Parton, " New Eskom board's 75% energy availability factor mandate is impossible, says Mark Swilling," News24, 24 October 2022. Available at: https://www.news24.com/fin24/economy/new-eskom-boards-75-energy-availability-factor-mandate-is-impossible-dbsa-chair-20221024. Accessed on 29 April 2023. (2023)

APPENDICES

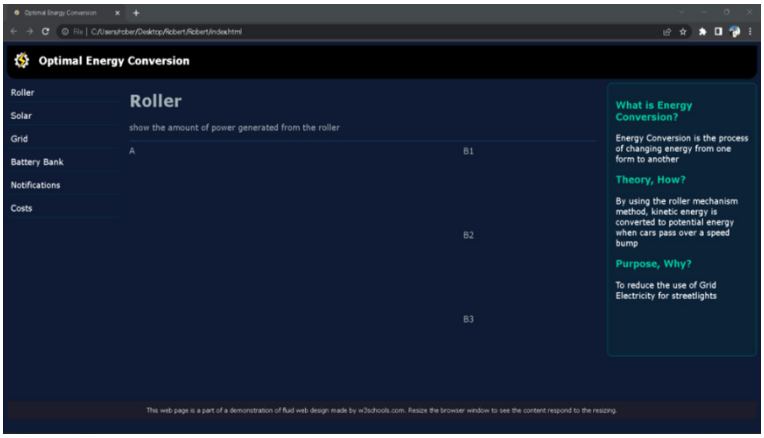

Appendix A. Website for ThingSpeak Results

Appendix B. Serial Communication Notification via SMS.

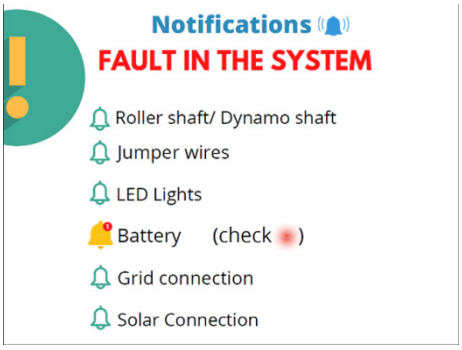

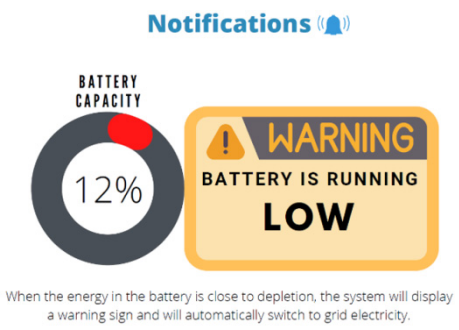

Appendix C. Fault in the system notification.